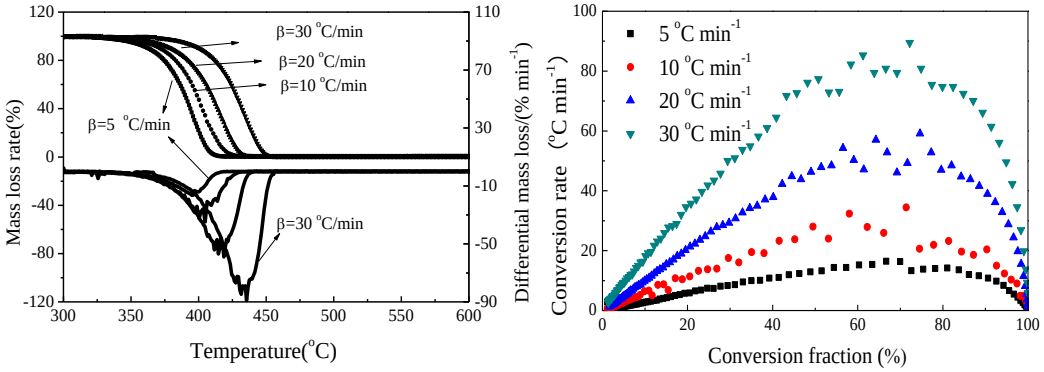

Fig.S1 The TG and DTG curves of typical medical waste pyrolysis

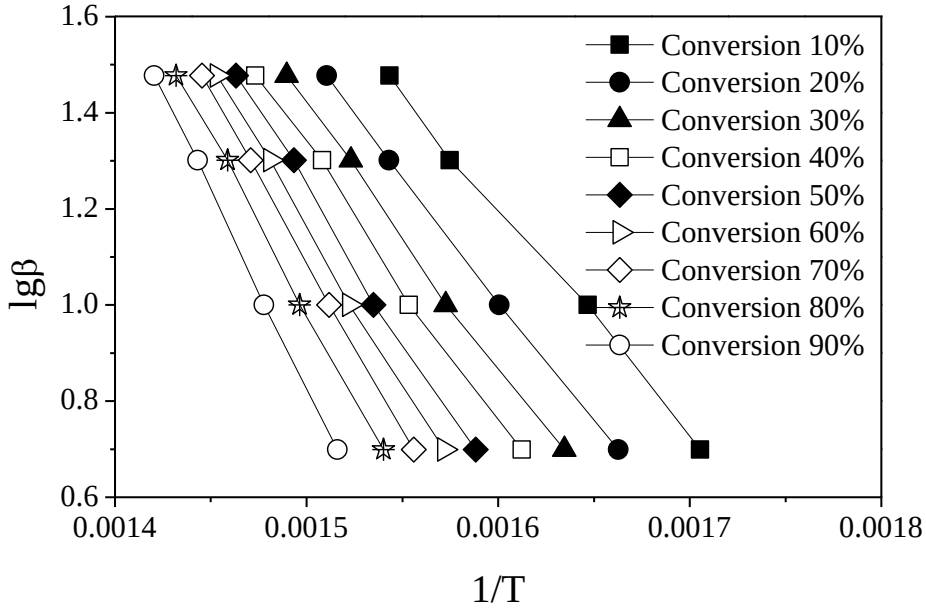

Fig. S2 The correlation of lgβ versus 1/T at different conversion

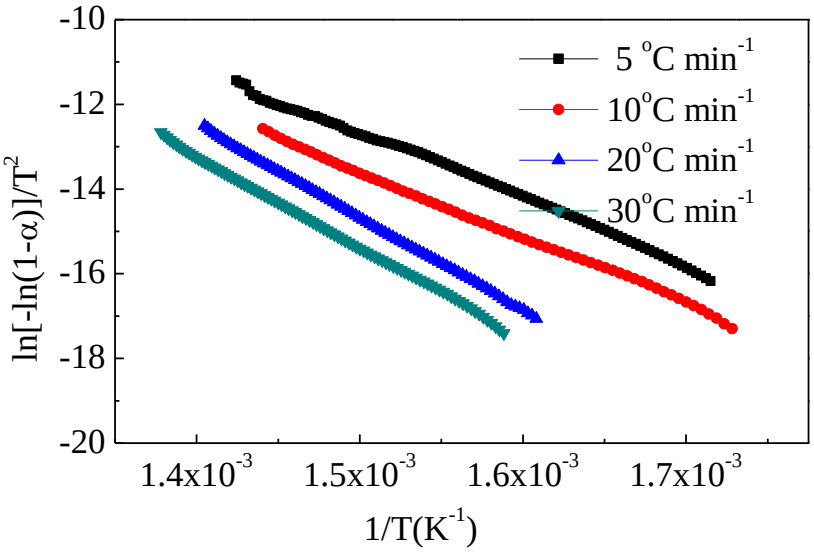

Fig. S3 The correlation of $\ln[-\ln(1-\alpha)]/T^2$ versus 1/T at different heating rate

Table S1 Most common reaction models for heterogeneous reaction.

Symbol	Reaction mechanism	f(x)	G(x)
G1	One-dimensional diffusion	$1/2x$	x^2
G2	Two-dimensional diffusion (Valensi)	$[-\ln(1-x)]^{-1}$	$x+(1-x)\ln(1-x)$
G3	Three-dimensional diffusion (Jander)	$1.5(1-x)2/3[1-(1-x)1/3]^{-1}$	$[1-(1-x)1/3]^2$
G4	Three-dimensional diffusion (G-B)	$1.5[1-(1-x)1/3]^{-1}$	$1-2x/3-(1-x)^{2/3}$
G5	Three-dimensional diffusion (A-J)	$1.5(1+x)2/3[(1+x)1/3-1]^{-1}$	$[(1+x)1/3-1]^2$
G6	Nucleation and growth (n=2/3)	$1.5(1-x)\ [-\ln(1-x)]^{1/3}$	$[-\ln(1-x)]^{2/3}$
G7	Nucleation and growth (n=1/2)	$2(1-x)\ [-\ln(1-x)]^{1/2}$	$[-\ln(1-x)]^{1/2}$
G8	Nucleation and growth (n=1/3)	$3(1-x)\ [-\ln(1-x)]^{2/3}$	$[-\ln(1-x)]^{1/3}$
G9	Nucleation and growth (n=1/4)	$4(1-x)\ [-\ln(1-x)]^{1/3}$	$[-\ln(1-x)]^{1/4}$
G10	Autocatalytic reaction	$x\ (1-x)$	$\ln[x/(1-x)]$
G11	Mampel power law (n=1/2)	$2x^{1/2}$	$x^{1/2}$
G12	Mampel power law (n=1/3)	$3x^{2/3}$	$x^{1/3}$
G13	Mampel power law (n=1/4)	$4x^{3/4}$	$x^{1/4}$
G14	Chemical reaction (n=3)	$(1-x)^3$	$[(1-x)^{-2}-1]/2$
G15	Chemical reaction (n=2)	$(1-x)^2$	$(1-x)^{-1}-1$
G16	Chemical reaction (n=1)	$1-x$	$-\ln(1-x)$
G17	Chemical reaction (n=0)	1	x
G18	Contraction sphere	$3(1-x)^{2/3}$	$1-(1-x)^{1/3}$
G19	Contraction cylinder	$2(1-x)^{1/2}$	$1-(1-x)^{1/2}$

Note: A-J: Anti-Jander; G-B: Ginstling-Brounshtein.

Table S2 Probable reaction models and kinetics parameters for H_2 during medical waste pyrolysis in MFBR

Temperature	G(X)	G3	G7	G8	G16
700 °C	lnK(T)	-4.2131	-2.9917	-3.3326	-2.2624
	R^2	0.9178	0.7422	0.6755	0.9784
750 °C	lnK(T)	-4.0008	-2.7395	-3.0791	-2.0371
	R^2	0.9299	0.7797	0.7229	0.9348
800 °C	lnK(T)	-3.7593	-2.5059	-2.8525	-1.7934
	R^2	0.9053	0.7848	0.7378	0.9495
850 °C	lnK(T)	-2.9720	-1.7243	-2.1078	-0.9856
	R^2	0.9429	0.9355	0.8927	0.9850
900 °C	lnK(T)	-2.9041	-1.6476	-1.9668	-0.9522
	R^2	0.9823	0.9726	0.9293	0.9918
E_a (kJ·mol^{-1})		**68.84**	**72.34**	**69.96**	**69.39**
A (s^{-1})		**65.42**	**342.13**	**182.78**	**495.12**

Table S3 Probable reaction models and kinetics parameters for CH_4 during medical waste pyrolysis in MFBR.

Temperature	G(X)	G3	G7	G8	G16
700 °C	lnK(T)	-3.4082	-1.8637	-2.1345	-1.3471
	R^2	0.9103	0.896	0.8772	0.9214
750 °C	lnK(T)	-3.2416	-1.6650	-1.9303	-1.1023
	R^2	0.9144	0.9434	0.9346	0.9419
800 °C	lnK(T)	-2.8860	-1.4254	-1.6933	-0.8620
	R^2	0.9422	0.9650	0.9138	0.9923
850 °C	lnK(T)	-2.6941	-1.2758	-1.5736	-0.7189
	R^2	0.9527	0.8991	0.8466	0.9646
900 °C	lnK(T)	-2.5718	-1.1855	-1.6140	-0.4805
	R^2	0.9809	0.9660	0.9312	0.9954
E_a (kJ·mol^{-1})		**42.29**	**33.34**	**27.01**	**40.21**
A (s^{-1})		**6.05**	**9.68**	**3.50**	**37.50**

Table S4 Probable reaction models and kinetics parameters for C_2H_2 during medical waste pyrolysis in MFBR

Temperature	G(X)	G3	G7	G8	G16
700 °C	lnK(T)	-2.7333	-1.7649	-1.8669	-0.8151
	R^2	0.9260	0.9596	0.9360	0.9595
750 °C	lnK(T)	-2.5145	-1.3224	-1.6414	-0.5490
	R^2	0.9652	0.9684	0.9355	0.9991
800 °C	lnK(T)	-2.3666	-1.0255	-1.3637	-0.4917
	R^2	0.9348	0.9634	0.9011	0.9651
850 °C	lnK(T)	-2.0746	-0.6962	-1.1351	-0.3274
	R^2	0.9608	0.9240	0.8668	0.9805
900 °C	lnK(T)	-1.6863	0.5322	-0.9115	-0.0483
	R^2	0.9260	1.0000	0.9833	0.9338
E_a (kJ·mol^{-1})		**47.60**	**59.05**	**45.85**	**33.16**
A (s^{-1})		**21.83**	**264.83**	**43.70**	**26.75**

Table S5 Probable reaction models and kinetics parameters for C_2H_4 during medical waste pyrolysis in MFBR

Temperature	G(X)	G3	G7	G8	G16
700 °C	lnK(T)	-3.7722	-2.4476	-2.7457	-1.8547
	R^2	0.9209	0.7937	0.7493	0.9347
750 °C	lnK(T)	-3.5032	-2.3046	-2.6145	-1.6836
	R^2	0.9227	0.8312	0.7836	0.9050
800 °C	lnK(T)	-3.2289	-1.9414	-2.4805	-1.4192
	R^2	0.9439	0.8617	0.7500	0.9103
850 °C	lnK(T)	-2.8932	-1.3591	-1.6363	-1.1725
	R^2	0.9864	0.9231	0.8626	0.9995
900 °C	lnK(T)	-2.6607	-1.0876	-1.1815	-1.0350
	R^2	0.9783	0.8977	0.8672	0.9707
E_a (kJ·mol^{-1})		**53.69**	**69.01**	**76.60**	**40.82**
A (s^{-1})		**16.99**	**380.20**	**662.82**	**23.61**

Table S6 Probable reaction models and kinetics parameters for C_2H_6 during medical waste pyrolysis in MFBR

Temperature	G(X)	G3	G7	G8	G16
700 °C	lnK(T)	-3.4577	-2.6145	-2.9662	-1.7418
	R^2	0.8921	0.7779	0.7263	0.8977
750 °C	lnK(T)	-3.2493	-2.2164	-2.5587	-1.4714
	R^2	0.9221	0.8025	0.7437	0.9142
800 °C	lnK(T)	-2.9169	-1.6079	-2.1733	-1.1963
	R^2	0.9558	0.9082	0.8508	0.9684
850 °C	lnK(T)	-2.7105	-1.4749	-1.8432	-0.9787
	R^2	0.9523	0.8771	0.8419	0.9427
900 °C	lnK(T)	-2.6105	-1.1466	-1.7131	-0.8470
	R^2	0.9997	0.9484	0.9041	1.000
E_a (kJ·mol^{-1})		**42.61**	**70.23**	**61.58**	**43.54**
A (s^{-1})		**6.10**	**443.01**	**107.90**	**38.65**

Table S7 Probable reaction models and kinetics parameters for C_3H_6 during medical waste pyrolysis in MFBR

Temperature	G(X)	G3	G7	G8	G16
700 °C	lnK(T)	-3.4610	-2.3166	-2.6479	-1.4784
	R^2	0.9414	0.8201	0.7528	0.9240
750 °C	lnK(T)	-3.2416	-1.9980	-2.2946	-1.2870
	R^2	0.9571	0.8782	0.7978	0.9600
800 °C	lnK(T)	-2.9858	-1.4974	-1.7778	-1.0527
	R^2	0.9458	0.9525	0.8958	0.9727
850 °C	lnK(T)	-2.7536	-1.3171	-1.7209	-0.8160
	R^2	0.9340	0.9951	0.9757	0.9667
900 °C	lnK(T)	-2.5536	-1.0692	-1.3677	-0.5989
	R^2	0.8737	0.9859	0.9905	0.9650
E_a (kJ·mol^{-1})		**43.69**	**60.58**	**59.80**	**42.21**
A (s^{-1})		**6.81**	**177.81**	**117.9**	**40.64**

Table S8 Probable reaction models and kinetics parameters for C_3H_8 during medical waste pyrolysis in MFBR

Temperature	G(X)	G3	G7	G8	G16
700 °C	lnK(T)	-5.8781	-4.5952	-5.0056	-4.0063
	R^2	0.9208	0.9870	0.9771	0.9634
750 °C	lnK(T)	-5.5468	-4.3351	-4.7330	-3.6969
	R^2	0.9615	0.9588	0.9171	0.9883
800 °C	lnK(T)	-5.3602	-4.2687	-4.6777	-3.4389
	R^2	0.9724	0.9478	0.9128	0.9818
850 °C	lnK(T)	-5.0207	-3.9954	-4.4228	-3.2289
	R^2	0.9953	0.9183	0.8813	0.9747
900 °C	lnK(T)	-4.8159	-3.4142	-3.8444	-2.8896
	R^2	0.9947	0.9104	0.8701	0.9815
E_a (kJ·mol^{-1})		**50.32**	**50.47**	**49.20**	**51.19**
A (s^{-1})		**1.41**	**4.76**	**2.72**	**10.08**

Table S9 Probable reaction models and kinetics parameters for C_4H_4 during medical waste pyrolysis in MFBR

Temperature	G(X)	G3	G7	G8	G16
700 °C	lnK(T)	-4.7330	-3.8258	-2.0341	-0.7221
	R^2	0.9043	0.7963	0.7241	0.9335
750 °C	lnK(T)	-4.5854	-3.4327	-1.5385	-0.5295
	R^2	0.9402	0.8748	0.7940	0.9582
800 °C	lnK(T)	-4.4567	-3.2089	-1.0131	-0.03542
	R^2	0.9826	0.9514	0.8944	0.9724
850 °C	lnK(T)	-3.8680	-2.9604	-0.9524	0.2937
	R^2	0.9855	0.9951	0.9757	0.9667
900 °C	lnK(T)	-3.4673	-2.7303	-0.6079	0.4448
	R^2	0.9755	0.9844	0.9905	0.9909
E_a (kJ·mol^{-1})		**60.70**	**50.74**	**65.85**	**60.02**
A (s^{-1})		**13.61**	**11.95**	**484.73**	**770.93**

Table S10 Probable reaction models and kinetics parameters for mixed gas during medical waste pyrolysis in MFBR

Temperature	G(X)	G3	G7	G8	G16
700 °C	lnK(T)	-4.8158	-2.9759	-3.4577	-2.6310
	R^2	0.9395	0.9927	0.9687	0.9696
750 °C	lnK(T)	-4.5375	-2.6200	-3.3326	-2.3309
	R^2	0.9748	0.9748	0.9231	0.9868
800 °C	lnK(T)	-4.2831	-2.6245	-3.1820	-2.1421
	R^2	0.9679	0.9472	0.8964	0.9933
850 °C	lnK(T)	-4.0513	-2.0129	-2.9431	-1.7418
	R^2	0.9778	0.9327	0.8738	0.9942
900 °C	lnK(T)	-3.7507	-1.7441	-2.8150	-1.5177
	R^2	0.9768	0.9663	0.8123	0.9560
E_a (kJ·mol^{-1})		**49.56**	**57.82**	**31.65**	**53.30**
A (s^{-1})		**3.64**	**61.27**	**1.52**	**50.79**